



Fabrication of Multifunctional $(\text{Co}_x^{2+}\text{Fe}_{1-x}^{2+})(\text{Al}_y^{3+}\text{Fe}_{2-y}^{3+})\text{O}_4$ Ferrite @ Graphene Oxide@Titania and Its Biological Activities

E. KALA[✉], M. YOGAPRIYA^{*}, P. VASANTHI[✉] and S. CHITRARASU[✉]

Department of Chemistry, Kalaignar Karunanidhi Government Arts College, Tiruvanamalai-600603, India

*Corresponding author: E-mail: yogapriyam@gmail.com

Received: 20 December 2023;

Accepted: 16 March 2024;

Published online: 31 May 2024;

AJC-21632

Recently, a variety of metal oxide-based nanomaterial has been integrated in several applications and achieved excellent performances on cyclic capacitor, antibacterial, antifungal and antioxidant activities. Titania doped cobalt aluminium ferrite fabricated graphene oxide based nanocomposites have received much attention. In this work, cobalt aluminium ferrite $(\text{Co}_x^{2+}\text{Fe}_{1-x}^{2+})(\text{Al}_y^{3+}\text{Fe}_{2-y}^{3+})\text{O}_4$ @ graphene oxide@titania nanocomposite was prepared at different ratios exhibiting the enhanced properties. Initially, the ferrite nanoparticles $(\text{Co}_x^{2+}\text{Fe}_{1-x}^{2+})(\text{Al}_y^{3+}\text{Fe}_{2-y}^{3+})\text{O}_4$ spinel ($0 \leq x$ and $y \geq 2$) ($x = 0, 0.2, 0.4, 0.6, 0.8, 1.0$ and $y = 1.0, 0.8, 0.6, 0.4, 0.2, 0$) powder were synthesized by substitution of A- and B-sites *via* sol-gel method using citrate as precursor. The obtained powder was calcined at 800 °C for 4 h. The coating of graphene oxide was done through solvothermal hydrolysis and powder obtained was calcined at 600 °C for 2 h followed by the second coating of titania was also performed similarly. The obtained multifunctional ferrite also showed potential antibacterial activity against Gram-negative bacteria (*Escherichia coli*) as well as Gram-positive bacteria (*Staphylococcus aureus*). The synthesized multifaceted spinel ferrites also showed moderate antioxidant activity of 59%.

Keywords: Spinal ferrite, Graphene oxide, Titania, Nanocomposites, Biological activities.

INTRODUCTION

In today's society, there is a rising and compelling need for environmental friendly high-power storage options. Super capacitors have attracted great attention on high power energy and outstanding cycling stability [1]. Recently, several metallic magnetic nanocrystalline of uniform particle size have been fabricated [2]. Cobalt ferrite and its substituted analogues hold significant technological significance across different fields. The utilization of coatings on graphene oxide and titania has gained significant attention in various applications [3,4]. One prominent strategy involves the application of coatings by the synthesis of graphene oxide and titania utilizing the solvothermal process [5-7].

It is reported that dosage amount of cobalt aluminium ferrite-graphene oxide-titania ferrite system increased the physical and chemical structural properties [8,9]. Spinal ferrite $(\text{Co}_x^{2+}\text{Fe}_{1-x}^{2+})(\text{Al}_y^{3+}\text{Fe}_{2-y}^{3+})\text{O}_4$ have attracted interest to many applications, substitution of Fe^{3+} ions with Al^{3+} ions in +III oxidation state [10] and Fe^{2+} ions with Co^{2+} ions in +II oxidation state [11], the ferrite

has been proposed as a method to induce interesting structural properties.

Due to the small size and strong magnetic features of cobalt ferrites result in their aggregation and limited photoinduced reactivity due to rapid photocarrier recombination, which adversely impacts their photocatalytic efficiency [12]. In addition, the incorporation of cobalt ferrite nanoparticles with graphene oxide has the advantage of tunable properties, a substantial surface area and a high electron mobility rate [13]. Simultaneously considerable attention has also been paid towards the structural, magnetic and electrical properties of some metal ion doped spinel ferrites [14-16]. The biological characteristics of ferrites are significantly influenced by their dimensions, morphology, polydispersity, charge and the composition of their coating [17,18]. Thus, keeping in mind about these points, in this article, aluminium substituted cobalt ferrite $(\text{Co}_x^{2+}\text{Fe}_{1-x}^{2+})(\text{Al}_y^{3+}\text{Fe}_{2-y}^{3+})\text{O}_4$ ($0 \leq x$ and $y \geq 2$) were obtained by a sol gel method and then the preparation and characterization of cobalt aluminium ferrite (magnetic core)@coating with GO (layer)@ coating with titania (photoactive shell) were carried out by direct coating

of titania using titanium isopropoxide as a titania precursor. Finally, the antimicrobial activity of prepared multifunctional ferrite against several pathogenic microorganisms were also carried out.

EXPERIMENTAL

Cobalt chloride hexahydrate ($\text{CoCl}_2 \cdot 6\text{H}_2\text{O}$), anhydrous iron chloride (FeCl_3), anhydrous citric acid ($\text{C}_6\text{H}_8\text{O}_7$), Millipore water, potassium permanganate, hydrogen peroxide 30% solution, titanium isopropoxide (TTIP) were procured from Merck Ltd. India. The other chemicals *viz.* anhydrous aluminium chloride (AlCl_3), ferrous chloride tetrahydrate ($\text{FeCl}_2 \cdot 4\text{H}_2\text{O}$) graphite fine powder, sulphuric acid, methanol were purchased from Loba Chemicals, India.

Synthesis of cobalt aluminium ferrite nanoparticle by sol-gel method (magnetic core): The $(\text{Co}_x^{2+}\text{Fe}_{1-x}^{2+})(\text{Al}_y^{3+}\text{Fe}_{2-y}^{3+})\text{O}_4$ spinel ($0 \leq x \text{ \& } y \leq 2$) ($x = 0, 0.2, 0.4, 0.6, 0.8, 1.0$ and $y = 1.0, 0.8, 0.6, 0.4, 0.2, 0$) powder were prepared by sol-gel method. The metal chlorides and citric acid as precursor were dissolved into Millipore water with homogeneous stirring. The pH value 7 was maintained by dropwise addition of 25% NH_3 solution. The formed sol-gel product was heated to 80°C on a hot plate with continuous stirring for 0.5 h and then upon condensation a xerogel was obtained, which further heated to 100°C finally to get ferrite powder. The powder was calcined for 4 h at 800°C to enhance the crystallinity. These samples are denoted as CA1-CA6.

Synthesis of graphene oxide coated ferrite nanoparticle by solvothermal method $[(\text{Co}_x^{2+}\text{Fe}_{1-x}^{2+})(\text{Al}_y^{3+}\text{Fe}_{2-y}^{3+})\text{O}_4@\text{GO}]$ (core/shell): Graphene oxide was synthesized by the modified Hummer method. Briefly, 20 g of graphite powder was added to conc. H_2SO_4 (500 mL) in a breaker at 0°C with continuous stirring followed by the addition of KMnO_4 (60 g) while maintaining the reaction temperature below 15°C . Then raised the reaction temperature to 35°C while stirring, the colour of the reaction changed to brown colour. The solution was then diluted with 1.5 L Millipore water to followed by addition of 20% of H_2O_2 and raised the reaction to 100°C for 0.5 h with continuous stirring. Finally, the solution was washed with Millipore water, acetone and 10% HCl in order to remove the residual metal ions. The product was filtered, dried in oven at 90°C for 24 h to obtain graphene oxide powder.

In next step, the graphene oxide coating on the synthesized cobalt aluminium ferrite was done by adding 1 g of GO and 1 g of ferrite powder in 250 mL of Millipore water. The solution was then ultrasonicated for 100 min at 90°C and after the removal of solvent, the powder sample was calcined at 600°C for 2 h to obtain coated cobalt aluminium ferrite@graphene oxide powder, which is denoted as CG1 to CG6.

Synthesis of titanium dioxide coated magnetic nanoparticle@GO by solvothermal method $[(\text{Co}_x^{2+}\text{Fe}_{1-x}^{2+})(\text{Al}_y^{3+}\text{Fe}_{2-y}^{3+})\text{O}_4@\text{GO}@\text{TiO}_2]$ (core/shell/shell): A colloidal TiO_2 solution and 2 mL titanium isopropoxide (TTIP) in 250 mL methanol were mixed with 1 g of CG1-CG6 powder while stirring at 60°C for 5 h and then ultrasonicated at 30°C for 100 min. Afterward, the solution was heated further to 80°C to evaporate the solvent and finally calcined at 600°C for 2 h to obtain cobalt

aluminium ferrite@GO@titania nanocomposite (CGT1 to CGT6) [19].

Characterization: The structural characterization of the prepared sample was performed using Philips X-ray diffractometer with Cu as the anode material. The UV-Vis absorption spectra of sample were acquired using a double beam ultraviolet-visible spectrophotometer using Jasco UV-Vis NIR instrument in the 200-800 nm range. The X-ray photoelectron spectroscopy (XPS) was used to determine the composition of the prepared samples using a PHI 5600ci spectrometer with an Al $K\alpha$ monochromatic X-ray source at 15 kV and 350 W. The IR spectra of the samples were recorded at room temperature in the range $4000\text{--}500\text{ cm}^{-1}$ using Alpha Bruker FT-IR instrument.

Antibacterial activity: The antibacterial activity was done using disc diffusion method. In brief, A 20 mL of Mueller Hinton agar were adjusted into sterile Petri dishes. The isolates and standardized bacterial stock suspension were adjusted to 0.5 McFarland and streaked on Mueller Hinton agar medium plates using a sterile cotton swab. Sterile filter paper discs (6 mm, Whatman No. 1) were soaked with different concentrations (12.5, 25, 50 and 100 mg/mL) of the prepared samples, and then placed on the surface of agar. The plates were then incubated for 24 h at 37°C and the diameters of the inhibition zones were measured in mm.

Antioxidant activity: The antioxidant activity of the prepared ferrites was assessed using the DPPH method. The concentrations of the coated ferrite nanocomposite (25, 50, 75, 100, and 125 $\mu\text{g/mL}$) were added to a 10 mL solution of 0.1 mM DPPH (Sigma-Aldrich, USA) and the mixture was then kept in the dark at room temperature for 0.5 h to allow the reaction to occur. Subsequently, the absorbance at a wavelength of 517 nm was measured using ethanol as a reference. The experiment was carried out in a similar manner using ascorbic acid (Sigma-Aldrich) as the reference standard.

RESULTS AND DISCUSSION

XRD studies: The XRD patterns of cobalt aluminium ferrite $(\text{Co}_x^{2+}\text{Fe}_{1-x}^{2+})(\text{Al}_y^{3+}\text{Fe}_{2-y}^{3+})\text{O}_4$ @graphene oxide@titania nanocomposites (CGT1-CGT6) is shown in Fig. 1. A strong crystalline peaks of graphene oxide were observed at 26° corresponding to the (002) plane of its hexagonal structure of graphite [20,21]. Moreover, a peak at 25° corresponds to anatase (101) plane of titanium isopropoxide (TTIP) crystallite of anatase (101) plane (JCPDS card no 21-1272), which confirmed the mesoporous structure formation [22]. In Co-Al-Fe oxide samples, all the diffraction planes were in good agreement with the $\alpha\text{-Fe}_2\text{O}_3$ hematite phase (rhombohedral) with JCPDS card No. 72-0469.

UV-Vis studies: Fig. 2 displays the UV-Vis spectra of cobalt aluminium ferrites nanocomposites as well as with doped with GO and titania nanocomposites. The cobalt, aluminium, iron and graphene showed more absorption the UV region but low absorption in the visible region. The band gap value of multifunctional coated ferrite nanocomposite was approximately ~ 1.7 to 2.8 eV as obtained by using Tauc plot (Fig. 2d) [23].

FT-IR studies: The FT-IR spectra of CGT1, CGT3 and CGT6 samples of cobalt aluminium ferrite@GO@titania is shown in Fig. 3. The band value in the range of 3745 cm^{-1}

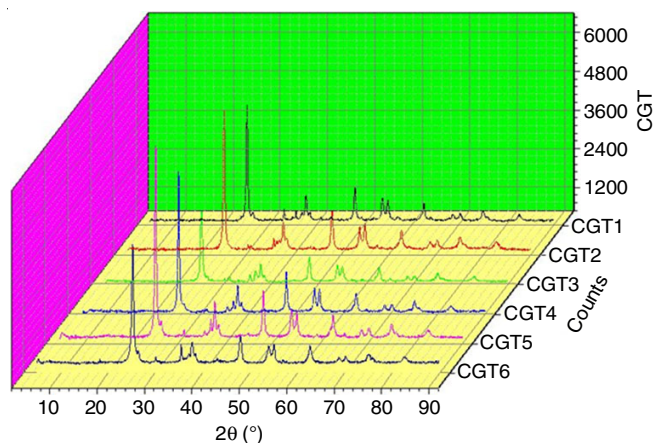


Fig. 1. XRD spectra of the prepared $(\text{Co}_x^{2+}\text{Fe}_{1-x}^{2+})(\text{Al}_y^{3+}\text{Fe}_{2-y}^{3+})\text{O}_4@GO@titania$ nanocomposites

corresponds to the OH groups. A peak at 2939 cm^{-1} is attributed to the carbon residual vibration, while the characteristic peaks

of graphene oxide were appeared at 2921 and 1034 cm^{-1} , however, the prepared nanocomposites display slightly different pattern in the region between 2000 to 400 cm^{-1} due to the presence of different metallic species. For example, a characteristic peak at $1035\text{--}1034\text{ cm}^{-1}$ corresponds to the FeO_2 species, while the absorption peaks at $1130\text{--}1123\text{ cm}^{-1}$ assigned to the $\nu(\text{Ti-O-C})$ bridging vibrations of isopropoxy groups [24–26].

XPS studies: The oxidation states of the elements and the oxygen vacancy with doping in the samples can be predicted from the images of XPS as shown in Fig. 4. Table-1 mentioned the binding energy values of Fe, Co, Al, O, C and Ti, which displays the peak value and FWHM (eV) values. From the high resolution spectrum of $\text{Co } 2p$, it can be seen that there are peaks at bonding energies of 775.61 eV and 775.61 eV (CGT3 and CGT6), corresponding to $^2p_{1/2}$ and $^2p_{3/2}$, respectively [27–29].

Antibacterial activity: The antibacterial results of the doped spinal ferrite against *E. coli* and *S. aureus* at $1\text{ }\mu\text{g/mL}$ (Fig. 5). In addition, the incorporation of coated spinal ferrite nanocomposites with carbon material, particularly graphene

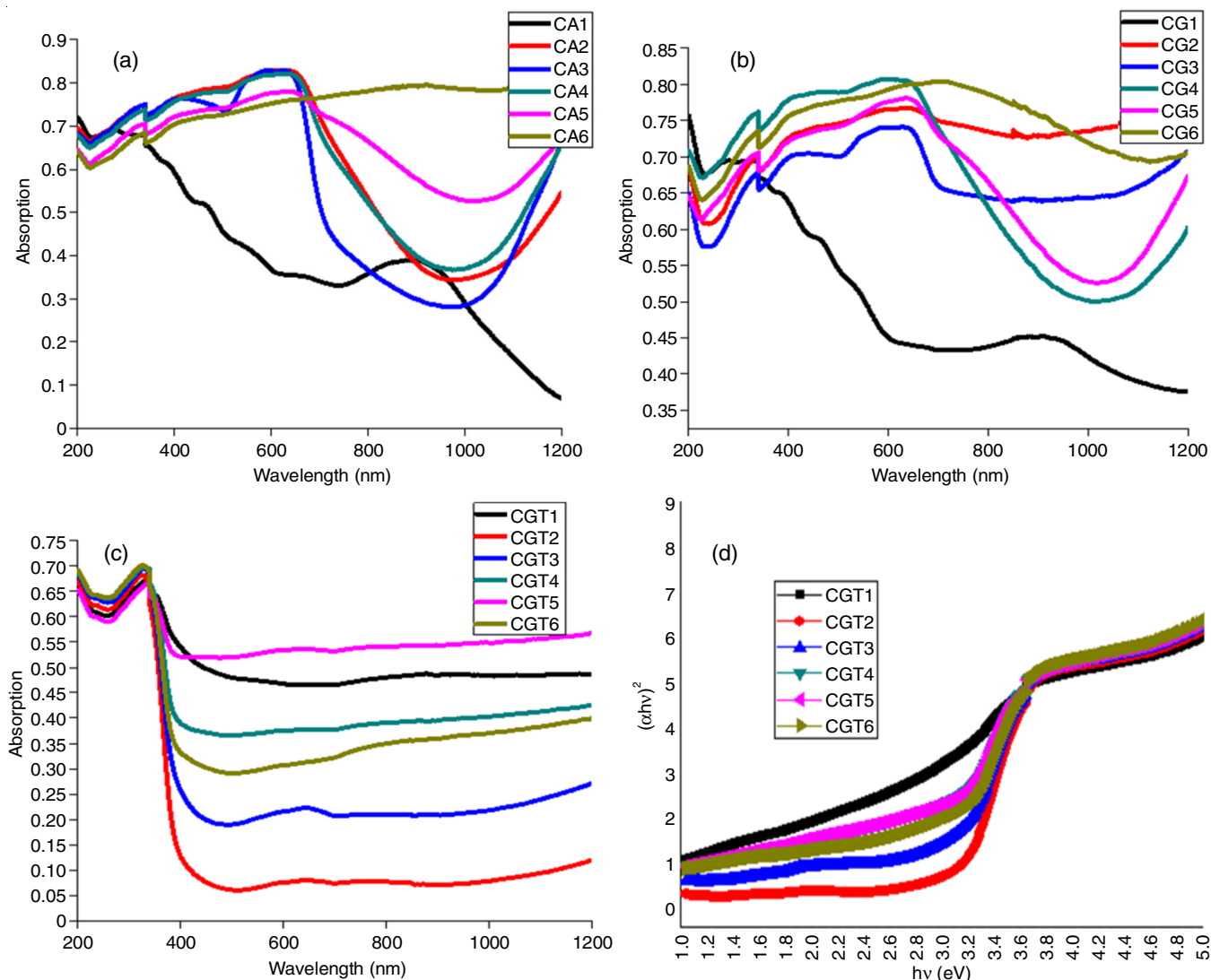


Fig. 2. UV-Visible spectra of cobalt aluminium ferrite nanoparticles (CA1-CA6) (a); $(\text{Co}_x^{2+}\text{Fe}_{1-x}^{2+})(\text{Al}_y^{3+}\text{Fe}_{2-y}^{3+})\text{O}_4@GO$ nanocomposites (CG1-CG6) (b); $(\text{Co}_x^{2+}\text{Fe}_{1-x}^{2+})(\text{Al}_y^{3+}\text{Fe}_{2-y}^{3+})\text{O}_4@GO@TiO_2$ nanocomposites (CGT1-CGT6) (c); and Tauc plots of $(\text{Co}_x^{2+}\text{Fe}_{1-x}^{2+})(\text{Al}_y^{3+}\text{Fe}_{2-y}^{3+})\text{O}_4@graphene\ oxide@TiO_2$ nanocomposites (CGT1-CGT6) (d)

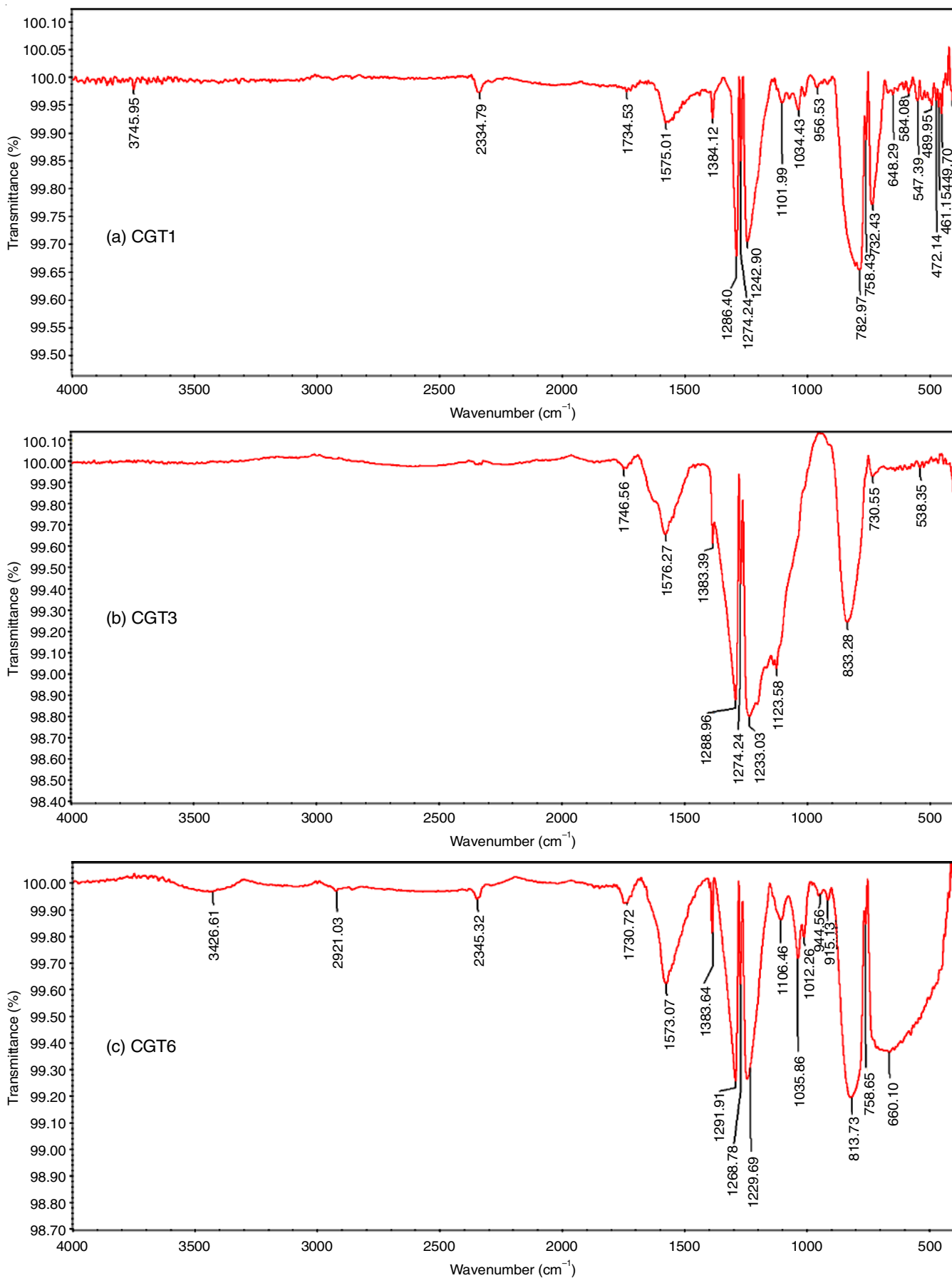


Fig. 3. IR spectra of some $(\text{Co}_x^{2+}\text{Fe}_{1-x}^{2+})(\text{Al}_y^{3+}\text{Fe}_{2-y}^{3+})\text{O}_4$ @GO@titania nanocomposites (a) CGT1, (b) CGT3 and (c) CGT6

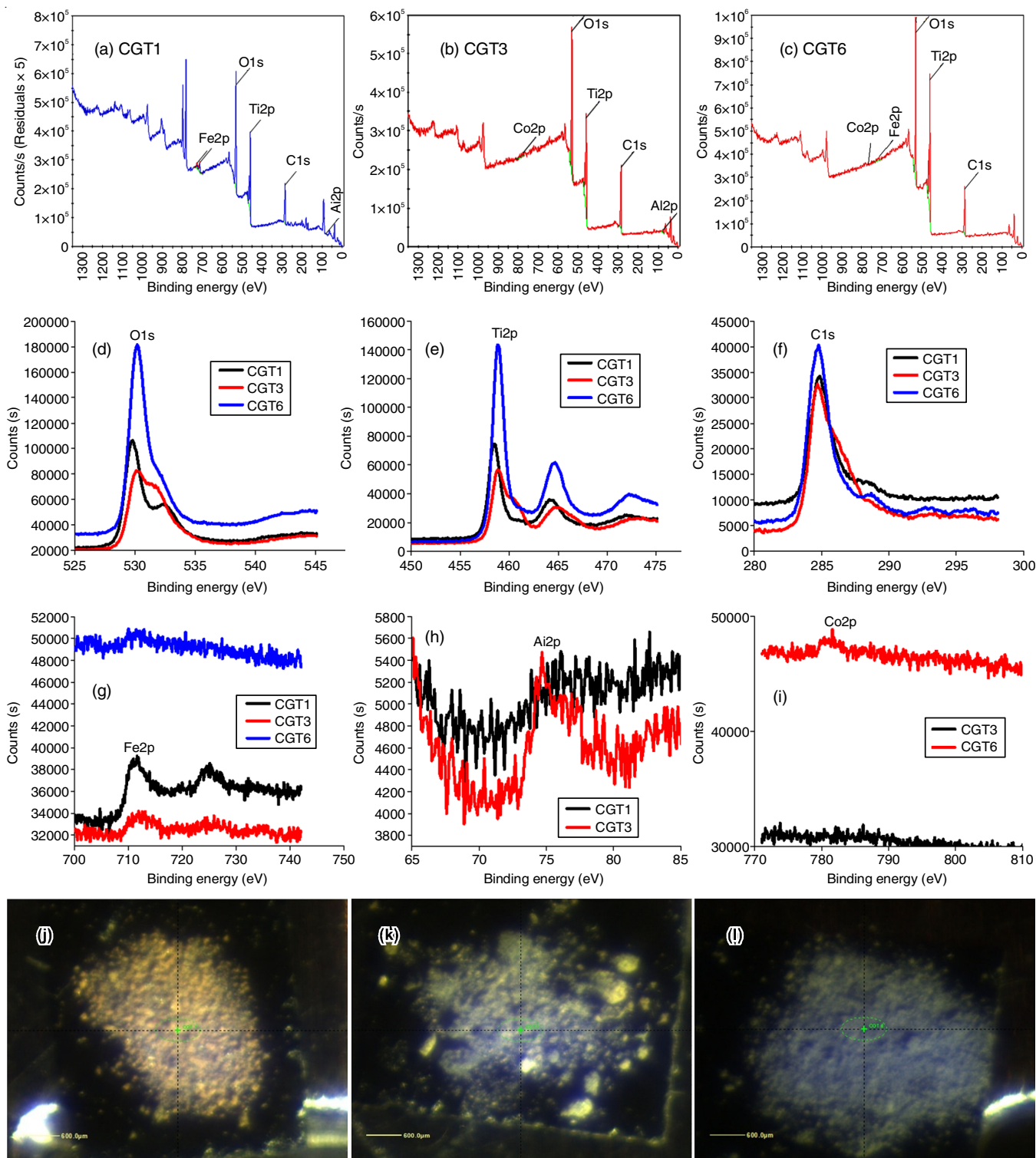


Fig. 4. XPS spectra of some $(Co_x^{2+}Fe_{1-x}^{3+})(Al_y^{3+}Fe_{3-y}^{3+})O_4@GO@titania$ nanocomposites and its scan images

TABLE-1
X-RAY PHOTOELECTRON SPECTROSCOPY BINDING ENERGY VALUES OF SYNTHESIZED DOPED SPINAL FERRITE NANOCOMPOSITES

Sample	C 1s		Ti 2p		O 1s		Fe 2p		Al 2p		Co 2p	
	Binding energy	FWHM (eV)										
CGT1	285.41	3.00	459.12	2.75	530.90	4.05	724.72	4.25	78.76	0.25	–	–
CGT3	285.83	3.52	459.54	1.85	531.27	3.87	724.72	4.25	78.76	2.24	775.61	1.32
CGT6	285.28	2.89	459.22	2.53	530.58	1.61	711.30	2.41	–	–	775.61	1.32

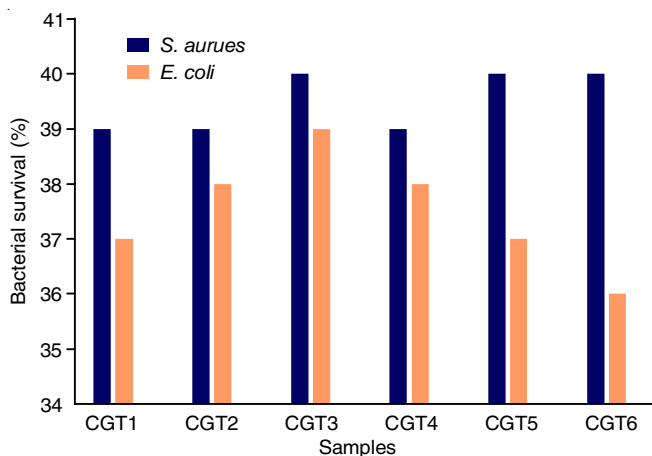


Fig. 5. Antibacterial activity of $(\text{Co}_x^{2+}\text{Fe}_{1-x}^{2+})(\text{Al}_y^{3+}\text{Fe}_{2-y}^{3+})\text{O}_4$ @GO@titania nanocomposites

oxide (GO), has the advantage of tunable properties, a substantial surface area and a high electron movement rate [30].

Antioxidant activity: It is evident from the results (Fig. 6) that synthesized coated spinal ferrite nanocomposites exhibited potent antioxidant activity at different concentrations, however, free radical scavenging activities of cobalt aluminium ferrite nanocomposites were inferior to the standard (ascorbic acid). With increased doses of spinal ferrites, the antioxidant activity was also increased accordingly upto 59%. This antioxidant activity could be linked to the transfer of free electrons of spinal ferrite nanocomposites to free radicals of DPPH molecules [31].

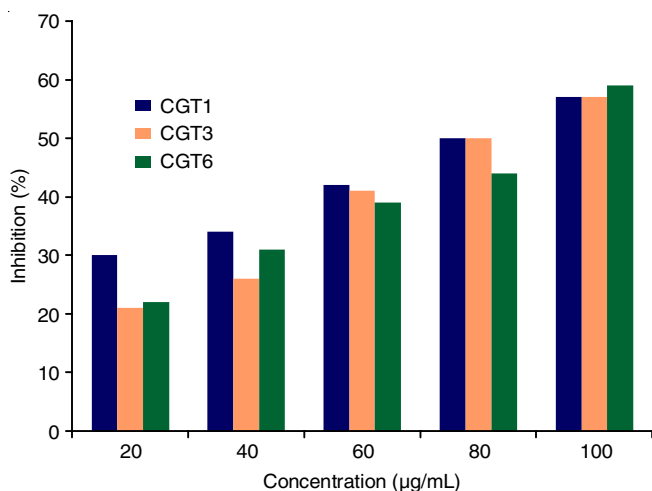


Fig. 6. Antioxidant activity of some $(\text{Co}_x^{2+}\text{Fe}_{1-x}^{2+})(\text{Al}_y^{3+}\text{Fe}_{2-y}^{3+})\text{O}_4$ @GO@titania nanocomposites

Conclusion

In this work, a multifaceted coated spinal ferrites *viz.* cobalt aluminium ferrite@graphene oxide@titania nanocomposites $(\text{Co}_x^{2+}\text{Fe}_{1-x}^{2+})(\text{Al}_y^{3+}\text{Fe}_{2-y}^{3+})\text{O}_4$ ($0 \leq x$ and $y \geq 2$) ($x = 0, 0.2, 0.4, 0.6, 0.8, 1.0$ and $y = 1.0, 0.8, 0.6, 0.4, 0.2, 0$) were synthesized, characterized and also evaluated its biological activity. Initially, cobalt aluminium ferrite was prepared *via* sol-gel method using citric acid as precursor. In order to enhance the structural

qualities, the coating of graphene oxide followed by the second coating of titania *via* solvothermal method was done. The powder XRD studies show the formation of cobalt aluminium-doped hematite of multiphase structure, while in the doped cobalt-spinal ferrite samples, all the diffraction planes were in good agreement with the α - Fe_2O_3 hematite phase (rhombohedral). Moreover, the spinal ferrites nanocomposite showed moderate antioxidant activity and besides, *in vitro* analysis also showed a moderate antibacterial activity on *E. coli* and *S. aureus*.

CONFLICT OF INTEREST

The authors declare that there is no conflict of interests regarding the publication of this article.

REFERENCES

- N. Kumar, S.-B. Kim, S.-Y. Lee and S.-J. Park, *Nanomaterials*, **12**, 3708 (2022); <https://doi.org/10.3390/nano12203708>
- L. Bai, Y. Ouyang, J. Song, Z. Xu, W. Liu, J. Hu, Y. Wang and F. Yuan, *Materials*, **12**, 1497 (2019); <https://doi.org/10.3390/ma12091497>
- M. Faraldos and A. Bahamonde, *Catal. Today*, **285**, 13 (2017); <https://doi.org/10.1016/j.cattod.2017.01.029>
- A. Aguilera-Mandujano and J. Serrato-Rodriguez, *Rev. Mex. Fis.*, **66**, 610 (2020); <https://doi.org/10.31349/revmexfis.66.610>
- S.J. Chin, M. Doherty, S. Vempati, P. Dawson, C. Byrne, B.J. Meenan, V. Guerrad and T. McNally, *Nanoscale*, **11**, 18672 (2019); <https://doi.org/10.1039/C9NR04202D>
- A.H. Mamaghani, F. Haghghat and C.-S. Lee, *Chemosphere*, **219**, 804 (2019); <https://doi.org/10.1016/j.chemosphere.2018.12.029>
- L. Ndlwana, N. Raleie, K.M. Dimpe, H.F. Ogotu, E.O. Oseghe, M.M. Motsa, T.A.M. Msagati and B.B. Mamba, *Materials*, **14**, 5094 (2021); <https://doi.org/10.3390/ma14175094>
- N. Abbas, J.-M. Zhang, M. Ikram, A.A. Ibrahim, S. Nazir, I. Ali, A. Mahmood and H. Akhtar, *Results Phys.*, **59**, 107576 (2024); <https://doi.org/10.1016/j.rinp.2024.107576>
- F.S. Alruwashid, M.A. Dar, N.H. Alharthi and H.S. Abdo, *Nanomaterials*, **11**, 2523 (2021); <https://doi.org/10.3390/nano11102523>
- A. Lassoued, M.S. Lassoued, B. Dkhil, S. Ammar and A. Gadri, *J. Mag. Magnet Mater.*, **476**, 124 (2019); <https://doi.org/10.1016/j.jmmm.2018.12.062>
- B. Ingale, D. Nadargi, J. Nadargi, R. Suryawanshi, H. Shaikh, M.A. Alam, M.S. Tamboli and S.S. Suryavanshi, *ACS Omega*, **8**, 30508 (2023); <https://doi.org/10.1021/acsomega.3c03757>
- A.M. El-Khawaga, Mohamed A. Elsayed, Y.A. Fahim and R.E. Shalaby, *Sci. Rep.*, **13**, 5353 (2023); <https://doi.org/10.1038/s41598-023-32323-y>
- A. Al Nafey, A. Addad, B. Sieber, G. Chastanet, A. Barras, S. Szunerits and R. Boukherroub, *Chem. Eng. J.*, **322**, 375 (2017); <https://doi.org/10.1016/j.cej.2017.04.039>
- B.A. Patil and R.D. Kokate, *Proc. Manufact.*, **20**, 147 (2018); <https://doi.org/10.1016/j.promfg.2018.02.021>
- V. Vaithyanathan, K. Ugendar, J.A. Chelvane, K.K. Bharathi and S.S.R. Inbanathan, *J. Magnet. Magn. Mater.*, **382**, 88 (2015); <https://doi.org/10.1016/j.jmmm.2015.01.052>
- A. Hao and X. Ning, *Front. Mater.*, **8**, 718869 (2021); <https://doi.org/10.3389/fmats.2021.718869>
- M. Colombo, S. Carregal-Romero, M.F. Casula, L. Gutierrez, M.P. Morales, I.B. Bohm, J.T. Heverhagen, D. Prospero and W.J. Parak, *Chem. Soc. Rev.*, **41**, 4306 (2012); <https://doi.org/10.1039/c2cs15337h>
- A. Sandhu, H. Handa and M. Abe, *Nanotechnology*, **21**, 442001 (2010); <https://doi.org/10.1088/0957-4484/21/44/442001>

19. M.D. Butterworth, S.A. Bell, S.P. Armes and A.W. Simpson, *J. Colloid Interface Sci.*, **183**, 91 (1996); <https://doi.org/10.1006/jcis.1996.0521>
20. Z.-J. Fan, W. Kai, J. Yan, T. Wei, L.-J. Zhi, J. Feng, Y. Ren, L.-P. Song and F. Wei, *ACS Nano*, **5**, 191 (2011); <https://doi.org/10.1021/nn102339t>
21. C. Nethravathi and M. Rajamathi, *Carbon*, **46**, 1994 (2008); <https://doi.org/10.1016/j.carbon.2008.08.013>
22. T. Szabo, O. Berkesi, P. Forgó, K. Josepovits, Y. Sanakis, D. Petridis and I. Dékány, *Chem. Mater.*, **18**, 2740 (2006); <https://doi.org/10.1021/cm060258+>
23. T. Solni, P. Ptacek, J. Másilko, J. Tkacz, E. Bartoněk, S. Davigsdóttir and R. Ambat, *Mater. Sci. Forum*, **851**, 153 (2016); <https://doi.org/10.4028/www.scientific.net/MSF.851.153>
24. K. Venkat Savunthari and S. Shanmugam, *J. Taiwan Inst. Chem. Eng.*, **101**, 105 (2019); <https://doi.org/10.1016/j.jtice.2019.04.042>
25. C. Ramesh, K. Maniyasundar and S. Selvanandan, *Mater. Today: Proc.*, **3**, 1569 (2016); <https://doi.org/10.1016/j.matpr.2016.04.044>
26. T. Saemian, M. Gharagozlou, M.H. Sadr and S. Naghibi, *J. Inorg. Organomet. Polym.*, **30**, 2347 (2020); <https://doi.org/10.1007/s10904-019-01406-7>
27. C.M. Magdalane, G.M.A. Priyadharsini, K. Kaviyarasu, A.I. Jothi and G.G. Simiyon, *Surf. Interfaces*, **25**, 101296 (2021); <https://doi.org/10.1016/j.surfin.2021.101296>
28. K. Khalid, A. Zahra, U. Amara, M. Khalid, M. Hanif, K. Mahmood, M. Aziz, M. Ajmal, M. Asif, K. Saeed, M.F. Qayyum and W. Abbas, *Chemosphere*, **338**, 139531 (2023); <https://doi.org/10.1016/j.chemosphere.2023.139531>
29. T. Tatarchuk, I. Mironyuk, V. Kotsyubynsky, A. Shyichuk, M. Myslin and V. Boychuk, *J. Mol. Liq.*, **297**, 111757 (2020); <https://doi.org/10.1016/j.molliq.2019.111757>
30. L. Zhang, L. Du, X. Yu, S. Tan, X. Cai, P. Yang, Y. Gu and W. Mai, *ACS Appl. Mater. Interfaces*, **6**, 3623 (2014); <https://doi.org/10.1021/am405872r>
31. S. Kanagesan, M. Hashim, S.A.B. Aziz, I. Ismail, S. Tamilselvan, N.B. Alitheen, M.K. Swamy and B.P.C. Rao, *Appl. Sci.*, **6**, 184 (2016); <https://doi.org/10.3390/app6090184>